Applied Food Research 6 (2026) 102032

Contents lists available at ScienceDirect

Applied Food Research

journal homepage: www.elsevier.com/locate/afres

Malva nut mucilage prepared by alkaline-aided extraction: Application as a co-structuring agent to enhance stability and encapsulation efficiency of alginate-based composite hydrogel

Nopparat Prabsangob [a,b,*], Sasithorn Hangsalad [a], Utai Klinkesorn [b,c], Tan Chin Ping [d]

[a] Department of Product Development, Faculty of Agro-Industry, Kasetsart University, Bangkok 10900, Thailand
[b] Research Unit on Innovative Technologies for Production and Delivery of Functional Biomolecules, Kasetsart University Research and Development Institute (KURDI), Bangkok 10900, Thailand
[c] Department of Food Science and Technology, Faculty of Agro-Industry, Kasetsart University, Bangkok 10900, Thailand
[d] Department of Food Technology, Faculty of Food Science and Technology, Universiti Putra, Selangor 43400, Malaysia

ARTICLE INFO

Keywords:
Alginate
Alkaline-assisted extraction
Antioxidant
Composite hydrogel
Encapsulation
Malva nut mucilage
Reishi extract

ABSTRACT

The alginate (Alg) hydrogel with health promoting effect was fabricated using malva nut mucilage (MNM) as co-structuring agent and Reishi extract (RE) as encapsulated compound. Firstly, effect of MNMs extracted by alkaline solutions at varying concentrations (i.e., 0, 0.05, and 0.1 M) as co-structuring agent for preparation of composite Alg based hydrogel was observed. Alkaline condition could elevate MNM extractable yield along with increased solubility of the derived mucilage. Incorporation of the alkaline extracted MNMs led to enhanced microstructure of the hydrogels expected since preferably interaction between Alg and the alkaline treated MNMs with more exposed functional groups. The MNMs extracted by 0.05 M NaOH ($MNM_{0.05\ M}$) was selected for mixing with Alg at different ratios (i.e., Alg:$MNM_{0.05\ M}$ of 3:1, 2:1, and 1:1) to fabricate the composite hydrogels. The mucilage promoted formability and improved microstructure of the hydrogels. Using Alg:$MNM_{0.05\ M}$ at 2:1 could prepare the composite hydrogel with enhanced stability without disturbing effect on thermal property of the hydrogels. Then, the composite hydrogels were loaded with RE at varying contents (i.e., 1, 2.5, and 5 % to produce RE-1, RE-2.5, and RE-5 hydrogels, respectively). Encapsulation efficiency (EE) of the hydrogels was improved with the added RE content: The EE of ca. 55.6, 60.3, and 61.3 % for RE-1, RE-2.5, and RE-5 hydrogels, respectively. The RE loaded hydrogels showed heat tolerance and improved stability under varying pH conditions. Additionally, the beads exhibited competent phenolic retainability even in a harsh acidic condition of simulated stomach and effective phenolic compound releasing in a simulated intestinal condition.

1. Introduction

There is a growing interest in functional foods with health promoting effects. Reishi or Lingzhi (*Ganoderma lucidum*) is an edible mushroom widely consumed in Asia countries, owing to availability of various bioactive compounds, including polyphenols, triterpenoids, amino acids, nucleotides, and polysaccharides (Ahmad et al., 2021). Global consumption of Reishi, especially in an extract form, has been steadily increasing due to health benefits in enhancing immune system and mitigating chronic diseases like diabetes and cancer (Ahmad et al., 2021). However, Reishi extract (RE) has a bitter taste associated with a pungent feeling factor and mushroomy after taste that limit its application in food products (Chuensun et al., 2024). The bioactive compounds present in the extract always easily degrade during processing and storing due to their susceptibility to some factors such as heating and the presence of oxygen. Loss of bioactive compounds can also occur during digestion, particularly in the acidic environment of the stomach, leading to reduced bioactivity of the compounds (Cai et al., 2020). To address these challenges, encapsulation is a promising approach to enhance stability and control release of the bioactive compounds.

Hydrogels are an interesting system for encapsulating bioactive compounds, attributed to the ease formation by using food grade hydrocolloids under mild and safe conditions (Paulo & Santos, 2020). Alginate (Alg) is commonly used for hydrogel formation due to its efficiency, safety, and availability. Alginate hydrogel can encapsulate

* Corresponding author at: Department of Product Development, Faculty of Agro-Industry, Kasetsart University, Bangkok 10900, Thailand.
E-mail address: faginrpr@ku.ac.th (N. Prabsangob).

https://doi.org/10.1016/j.afres.2026.102032
Received 6 February 2026; Received in revised form 6 April 2026; Accepted 20 April 2026
Available online 21 April 2026

various compounds such as plant phenolic extracts (Benković et al., 2021; Flamminii et al., 2020), enzymes (Martín et al., 2019) and medicines (Rezvanian et al., 2017). However, the Alg gel matrix possess structural fragile with high porosity, so the encapsulated compounds tend to be easily released from the gel matrix, making difficulty of control release of the compounds (Jing et al., 2025; Mirmazloum et al., 2021; Neuenfeldt et al., 2021). With high porosity, approaching of oxygen, bile salts, and digestive enzyme is preferable, resulting in degradation of the enveloped compounds (Jing et al., 2025; Mousavi et al., 2020). Moreover, the Alg-based gel is always acid labile, resulting in limited encapsulation efficiency of the Alg-based hydrogel, particularly in the human stomach with high acidity (Doumèche et al., 2004; Ramdhan et al., 2020). These limitations lead to restricted application of the Alg-based hydrogel as bioactive compound vehicle model.

To reinforce the Alg gel matrix, proteins such as whey (Flamminii et al., 2020), gelatin (Tu et al., 2015), and soy protein isolate (Zhang et al., 2015), are the most widely employed as a co-structuring agent with Alg, owing to the excellent biocompatibility of the protein-polysaccharide combination (Flamminii et al., 2020; Li et al., 2019; Tu et al., 2015; Zhang et al., 2015). However, proteins might be susceptible to protease in the human gastrointestinal tract, leading to less control release of the encapsulated compounds (Li et al., 2019). Plant polysaccharide is interesting candidate to improve stability and encapsulation efficacy of hydrogel, owing to its technological and bioactive properties as well as an increasing trend of plant-based food consumption (Chen et al., 2022; Huang et al., 2019). Malva nut mucilage (MNM), the polysaccharides extracted from the nut of *Scaphium scaphigerum* which is an indigenous plant of Southeast Asia, has traditionally been consumed for their health promoting effects such as antioxidant property (Phlicharoenphon et al., 2018), laxative, and starch digestive enzyme inhibition effects (Srichamroen & Chavasit, 2011a). With its hydrophilicity, MNM possesses functional properties such as water retainability and gelling ability (Srichamroen & Chavasit, 2011b) that may enhance formation and encapsulation efficacy of the Alg-based hydrogel. Extraction method crucially affects characteristics of plant polysaccharide, thereby determining dissimilar functional properties of the derived compound. Hot-water extraction is generally performed for polysaccharide recovery from plant materials, in which some drawbacks are often observed such as low extractable yield, long extraction time, and restricted functional properties of the received polysaccharides (Chen et al., 2022, 2022). Alklaine-assisted extraction might promote recovery yield and functional properties of the polysaccharides attributed to the effect of alkaline to enhance a breakdown of chemical bonds in plant cellular matrix (Chen et al., 2022). Extraction using 1 % and 5 % NaOH solutions led to improved recovery yield of the polysaccharides from longan pulp (Huang et al., 2019) and flaxseed (Hellebois et al., 2021), respectively. Alkaline-aided extraction also led to elevated yield along with antioxidant capacity of the polysaccharide from mung bean skin (Chen et al., 2022). Considering MNM, it has been previously reported that alkaline extraction could promote gelling property of the mucilage (Srichamroen & Chavasit, 2011b), but the data on functional property of the mucilage as a co-structuring agent for Alg-based gel formation has not been elucidated yet.

This study aimed to fabricate the composite Alg-based hydrogels loaded with the antioxidative RE by using MNM as a co-structuring agent to promote stability and control release of the hydrogels. Firstly, the effect of alkaline–aided extraction on characteristics of MNM employed as a co-structuring agent with Alg to prepare the composite hydrogel was observed. After determining appropriate extracting condition to prepare MNM, the mixing ratio between Alg and the selected MNM for the composite hydrogel formation was elucidated. Finally, the composite hydrogels loaded with RE at varying contents were prepared to reveal their stability and releasing behavior through the *in vitro* digestive model. Overall results from the present work may elucidate feasible utilization of the Alg-MNM hydrogels loaded with bioactive compounds for the development of food with health-promoting effect.

2. Materials and methods

2.1. Materials

Malva nuts were purchased from a local market (Bangkok, Thailand). Reishi extract (RE) from the fruiting body of *Ganoderma lucidum* was a product of Specialty Natural Products Co. Ltd. (Chonburi, Thailand). Sodium-alginate (CAS No. 9005-38-3); calcium-lactate (CAS No. 5743-47-5); and Folin Ciocalteu's phenol reagent (CAS No. 12111-13-6) were purchased from LOBA Chemie Pvt Ltd. (New Delhi, India). NaOH (CAS No. 1310-73-2) was the product of KemAus (NSW, Australia). Digestive components, including porcine pancreas α-amylase Type VI-B ($\geq$ 5 U/mg; CAS No 9000-90-2), porcine gastric mucosa pepsins ($\geq$ 250 U/mg; CAS No 9001-75-6), porcine pancreas lipase (100–650 U/mg protein using olive oil as a substrate; CAS No 9001-62-1), and porcine bile extract (CAS No 8008-63-7) were products of Sigma-Aldrich Chemical Co. (MO, USA). All reagents were of analytical grade.

2.2. Property of crude gum prepared from Malva nut using different extracting solutions

Extraction of the gum was conducted following the method of Nuchchareonpaiboon and Prabsangob (2023) with some modifications. Initially, Malva nuts were soaked in dissimilar extracting solutions–i.e., de-ionized (DI) water, 0.05 M NaOH, and 0.1 M NaOH, – with a nut-to-water weight ratio of 1:25, at room temperature for 12 h. Subsequently, the seed and shell fractions were manually removed, and excess water was filtered out using a cheese cloth. The extracted gum was dried by hot-air oven (BWS model, Frecon, Bangkok, Thailand) at 60 $\pm$ 2 °C and air velocity of 1.0 m/s until the moisture content was lower than 10 %, before grinding using a blender (MX-EG5311, Panasonic Cooperation, Tokyo, Japan) and passed through the 60-mesh sieve. The gums derived were stored at 4 °C for less than 2 months before use. The crude gums extracted from Malva nut using DI water, 0.05 M NaOH, and 0.1 M NaOH were referred to as MNM_{0M}, $MNM_{0.05\ M}$, and $MNM_{0.1\ M}$, respectively. Property of the MNM samples were then characterized by measuring.

- ***Extraction yield:*** Extraction yield was estimated as a percentage of the gum derived to the weight of malva nut seed as a raw material.
- *Moisture and protein contents:* Moisture and protein contents were evaluated by a standard method (AOAC, 1990).
- *Swelling property and solubility index:* The extracted gum and distilled water were mixed in a centrifugal tube at a solid-to-liquid ratio of 1:100, heated at 80 °C for 30 min, and then cooled to room temperature. After centrifuging (5000 $\times$ g, 15 min), the supernatant was decanted in a pre-weighed petri dish. Increasing of the centrifuge tube weight was expressed as a swelling index, whereas increasing of the petri dish weight after heating (110 °C, 12 h) and cooling in a desiccator to room temperature was expressed as solubility index (Hamdani et al., 2018).
- *Water holding capacity (WHC) and oil holding capacity (OHC):* WHC and OHC of the MNM samples were determined by the method described by Wani et al. (2015) with some modification. The crude gum (W_1) was mixed with distilled water at a solid-to-liquid ratio of 1:20) at room temperature for 1 h. Then, the mixture was centrifuged (6500 $\times$ g, 10 min) to get rid of a supernatant. Different weights of sediment and crude gum were used to calculate the percentage of WHC based on the weight of crude gum. OHC was determined as per the WHC measurement method, but soybean oil was used instead of distilled water.
- *Structural characteristic:* Chemical structure of the MVG samples was analyzed using a Fourier transform infrared (FT-IR) spectrometer (Tensor 27, Bruker, Ettlingen, Germany) with 16 scans at 4 cm^{-1} resolution over the wavelength of 4000–500 cm^{-1} (Li et al., 2021).

2.3. Effect of MNMs prepared by different extracting solutions on Alg hydrogel formation

The MNMs derived from dissimilar extracting solutions were employed to prepare the hydrogels together with Alg through an ionotropic gelation method as described by Alex et al. (2013) with a slight modification. Alg and each MNM were thoroughly mixed at the weight ratio of 3:1 using DI water to prepare the solution with a fixed concentration of 1.5 %. The mixture was then introduced into a syringe (2 mm in diameter), and the hydrogels were introduced dropwise into an aqueous Ca-lactate solution (0.05 M). Hardening of the beads was accomplished by a gentle mixing for 15 min, followed by rinsing the beads with acetate buffer (0.1 M, pH 5.5). The hydrogels prepared using Alg without the MNM were regarded as a control. The hydrogels were stored at 4 °C for less than 2 weeks before measuring.

- *Spherical index (SI):* Size of the beads (at least 30 beads) was measured using a vernier caliper. SI was calculated based on the largest diameter (D_{max}) and smallest diameter (D_{min}) of the hydrogels as per the following equation (Chan et al., 2009).

$$SI = (D_{max} - D_{min})/(D_{max} + D_{min}) \quad (1)$$

- *Morphological characteristics:* Morphology of the hydrogels was assessed using a scanning electron microscope (Quanta 450, FEI Company, OR, USA) as per the method of Li et al. (2021). After freeze-drying, the beads were sputter-coated with gold before observing the cross section under 15 kV accelerating voltage.
- *Structural characteristic:* Chemical structure of the hydrogels was analyzed using a FT-IR spectrometer as the aforementioned procedure (Li et al., 2021).
- *Thermal property:* Thermal property of the hydrogels was characterized by a differential scanning calorimeter (204 F1 Phoenix, Netzsch-Gerätebau GmbH, Selb, Germany). The freeze-dried beads were finely ground and immediately sealed in an aluminum crucible. The samples were heated from 30 °C to 300 °C at a heating rate of 10 °C/min, with an empty aluminum crucible serving as a reference.
- *Bead strength:* Strength of the beads was assessed using texture profile analysis (TPA) following the method of Martín et al. (2019) with some modifications. The TPA analyzer (TA-XT2, Stable Micro Systems Ltd., Surrey, UK) equipped with a 5 kg load cell and a cylindrical probe (35 mm in diameter) was employed. The measurement was conducted at room temperature with at least 10 beads tested for each sample to determine the hardness of the hydrogels.

From this section, the extracting solution providing the MNM that could strengthen the Alg hydrogels was selected as a representative for a next study.

2.4. Effect of Alg:MNM ratio on hydrogel formation

The selected MNM was employed as a co-structuring agent to prepare Alg hydrogels at different Alg:MNM weight ratios of 3:1, 2:1, and 1:1 (dry basis) according to the aforementioned procedure. The Alg hydrogels prepared without the MNM were used as a control. The hydrogels were characterized as described previously. Additionally, the stability of the beads against heating and storing under different pH conditions was assessed.

- pH *stability:* The hydrogels were immersed in various buffer solutions, including citrate buffer (10 mM, pH 3.0), acetate buffer (10 mM, pH 5.0), and phosphate buffer (10 mM, pH 7.0), at ratio of 1:5 (wt/v). The soaked beads were kept at room temperature for one week, and bead stability was expressed as the relative change in the spherical index (ΔSI) after one week compared to the initial SI (Kurkuri & Aminabhavi, 2004).
- *Heating stability:* The hydrogels were submerged in DI water (1:5, wt/vol) and heated at 72 °C for different durations (1, 5, and 10 min). After cooling to room temperature, bead stability was expressed as ΔSI after heating compared to SI before heating (Kurkuri & Aminabhavi, 2004).

The suitable mixing ratio between Alg and MNM was established based on the stability of the hydrogels for further study.

2.5. Alg-MNM hydrogels for RE encapsulation

The hydrogels prepared using Alg and the MNM at the selected ratio were used to encapsulate RE at varying concentrations. Alg and the MNM, at the chosen weight ratio, were mixed in DI water before adding with RE at different contents (1, 2.5, and 5 % by weight of total polysaccharides). The total DI water content was adjusted by subtracting the weight of the used RE to maintain the formula across all samples. The hydrogels were prepared and characterized as previously described, and their efficiency in encapsulating RE was then observed by measuring.

- *Loading efficiency (LE) and encapsulation efficiency (EE):* The hydrogels were soaked in DI water at the ratio of 1:5 (wt/v), shaken in a water bath (WNB7L4, Memmert GmbH, Schwabach, Germany) at 37 °C for 6 h, and allowed to stand at room temperature for 12 h. The beads were then separated, and the soaking water was subjected for total phenolic content (TPC) measurement by the Folin-Ciocalteu assay (Singleton and Rossi (1965) using gallic acid as a standard. LE and EE were quantified as per the following equations, respectively (Alex et al., 2013).

$$LE\ (mg\ GAE\ /\ g\ bead) = (TPC_{int} - TPC_{soln})\ /\ weight\ of\ hydrogels \quad (2)$$

$$EE\ (\%) = [(TPC_{int} - TPC_{soln})\ /\ TPC_{int}] \times 100 \quad (3)$$

where TPC_{int} is the TPC of RE incorporated in the hydrogels, and TPC_{soln} is the TPC of the soaking solution after shaking.

2.6. Stability and in vitro gastrointestinal digestion on phenolic releasing of the hydrogels

Characteristics of the composite hydrogels loaded with RE at varying contents were further examined by determining bead stability during storage at varying pH and heating at different durations. Moreover, phenolic releasing from the beads was monitored through the *in vitro* model of simulated gastric and intestinal phases as following.

- pH *stability:* The hydrogels were immersed in different buffer solutions, including citrate buffer (10 mM, pH 3.0), acetate buffer (10 mM, pH 5.0), and phosphate buffer (10 mM, pH 7.0), at a ratio of 1:5 (*wt/vol).* After one week, TPC and DPPH radical scavenging ability of the beads were determined according to the methods of Singleton and Rossi (1965) and Brand-Williams et al. (1995), respectively. The relative change in TPC (ΔTPC) and DPPH radical scavenging ability (ΔDPPH radical scavenging ability) of the beads were calculate based on the alteration of TPC (DPPH radical scavenging ability) values measured after one week compared to the initial values of the beads as per the method modified from Wongverawattanakul et al. (2022).
- *Heating stability:* The hydrogels were immersed in DI water (1:5, wt/v) and heated at 72 °C for different durations (1, 5, and 10 min). After cooling to room temperature, ΔTPC and ΔDPPH radical scavenging

ability of the beads were calculated based on the measurement before and after heating.

- *In vitro phenolic releasing of the hydrogels:* The hydrogels loaded with RE were subjected to an *in vitro* digestion as per the method of Le et al. (2020) with some modifications. Firstly, simulated gastric fluid (SGF) and simulated intestinal fluid (SIF) were prepared: SGF contained KCl (6.9 mM), KH_2PO_4 (0.9 mM), $NaHCO_3$ (0.25 M), NaCl (0.47 M), $MgCl_2 \bullet 6H_2O$ (0.1 mM), and $(NH_4)_2CO_3$ (0.5 mM); and SIF contained KCl (6.8 mM), KH_2PO_4 (0.8 mM), $NaHCO_3$ (0.85 M), NaCl (0.38 M), $MgCl_2 \bullet 6H_2O$ (0.33 mM). The SGF and SIF were clear solutions with the pH of 2.5 and 7.0, respectively.

The hydrogels (10 g) were mixed with SGF (50 mL) and pepsins (25,000 unit/mL) and introduced to a shaking water bath at 37 °C for 2 h. The hydrogels were then separated and mixed with SIF (50 mL), pancreatic lipase (5600 unit/mL), and bile salts (0.10 M). The mixture was then adjusted to pH 7.0 using an aliquot of NaOH solution (1 M) and incubated in a shaking water bath at 37 °C for 4 h. During the simulated gastric and intestinal digestion, small aliquots of the digesta were periodically taken out to measure TPC, and SGF or SIF at the same volume were added to maintain the total volume of the mixture.

2.7. Statistical analysis

The samples were independently prepared in triplicate. The measurements were conducted in triplicate, and the mean values ± standard deviations were reported. Differences between the means were statistically assessed using analysis of variance at a confidence level of $p \leq 0.05$ (SPSS for Windows; SPSS Inc.; IL, USA).

3. Results and discussion

3.1. Property of MNMs prepared using different extracting solutions

Firstly, the property of the MNMs derived by using alkaline extracting solutions at dissimilar concentrations was determined, and the result is shown in Table 1. Increasing alkaline extracting solutions led to improved recovery yield of the derived mucilage. This trend was in accordance with the others and might be attributed since effect of the alkaline to promote disruption of chemical bonds between the components in plant cellular matrix, thereby enhancing polysaccharide liberation (Chen et al., 2022; Hellebois et al., 2021; Huang et al., 2019). Concentration of the alkaline extracting solutions had no significant effect on protein content of the derived mucilage. Using the extracting solutions at increased alkaline concentration led to the mucilage with lowered OHC, whereas WHC was not affected. This trend implied lowered hydrophobicity of the MNMs extracted by the alkaline solutions, which might be expected due to effect of the alkaline solutions to cleave polysaccharide into fractions with hydrophilic ends of hydroxyl and carboxyl residues (Sun et al., 2018). Increased concentration of the alkaline extracting solutions led to improved solubility of the derived MNMs, whereas effect on swelling property of the mucilage was not noticeable. Increase in solubility of the derived MNMs might be associated with the polysaccharide fractions with water interacting capacity (Hamdani et al., 2018). Due to γ-radiation treatment, solubility of guar gum and locust bean gum could be improved and supposed since greater fractionation of the polysaccharides induced by the radiation (Hamdani et al., 2018).

Table 1
Characteristics of the MNMs prepared by alkaline extracting solutions at different concentrations.

characteristic	MNM_{0M}	$MNM_{0.05M}$	$MNM_{0.1M}$
extraction yield (%)	22.53 ± 0.32^b	28.40 ± 0.43^a	29.41 ± 0.99^a
protein content (%, db)	0.11 ± 0.03	0.06 ± 0.04	0.07 ± 0.02
solubility (%)	42.13 ± 1.99^c	60.40 ± 2.08^b	71.66 ± 1.66^a
swelling property (g/g)	35.92 ± 7.57	34.69 ± 6.89	34.90 ± 7.68
WHC (g/g)	27.73 ± 1.22	26.62 ± 0.09	27.70 ± 1.19
OHC (g/g)	26.26 ± 0.42^a	14.54 ± 0.87^b	15.53 ± 0.62^b

In each row, different superscripts indicate difference between means ($p \leq 0.05$).

Fig. 1 depicted FT-IR profiles of the extracted MNMs. The spectra typically related to polysaccharides were observed for all samples which correlated well with others: These spectra included the peaks at ca. 3000–3500 cm^{-1} suggesting the presence of –OH group; the peaks at ca. 2800–3000 cm^{-1} representing stretching C–H bonds of methyl groups; the peaks at ca. 1600 cm^{-1} implying asymmetric stretching $–COO^-$ and symmetric stretching of carbonyl groups; the peaks at ca. 1410 cm^{-1} relating to the bending of C–H; and the peaks at ca. 1030 cm^{-1} implying a vibration of glycosidic C–O–C and C–O–H bonds (Apoorva et al., 2020; Flamminii et al., 2020). By employing dissimilar extracting solutions, the FT-IR spectra of the derived mucilage were affected. Extraction using the alkaline solutions at increased concentrations provided the mucilage showing increased intensity of the peaks at ca. 3000–3500 cm^{-1} and 1030 cm^{-1}, whereas the peak at ca. 1730 cm^{-1} disappeared. The peak at ca. 1730 cm^{-1} related to the presence of uronic acid (Lopez-Torrez et al., 2015). The present result, therefore, suggested degradation of uronic acid residues due to alkaline solution at increased concentration. Uronic acid was unstable and easily released due to hydrolysis reaction, so extraction using the alkaline solution at increased concentrations might led to degradation of uronic acid residues (Wang et al., 2016). The peak at ca. 3000–3500 cm^{-1} related to the inter– and intramolecular hydrogen bonds of glucuronic acid and galacturonic acid (Nep & Conway, 2011), whereas the peak at ca. 1000–1050 cm^{-1} could be expected since a presence of pyranose rings (Ying et al., 2011). Increased absorbances of the peaks at ca. 3000–3500 cm^{-1} and 1030 cm^{-1} of the alkaline extracted MNMs, therefore, might relate to more exposed

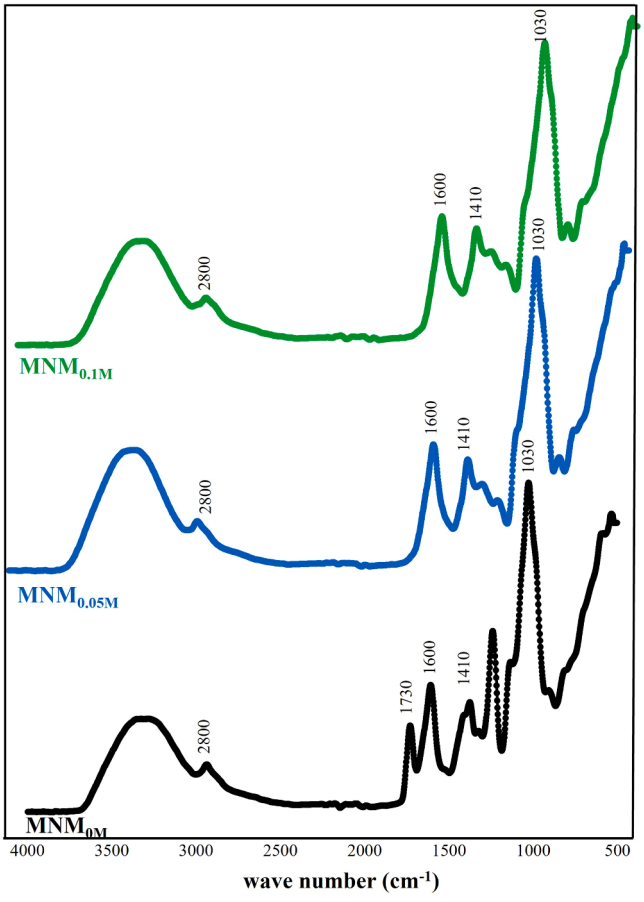

Fig. 1. FT-IR spectra of the MNMs prepared using different extracting solutions.

monosaccharide moieties of the cleaved polysaccharides with smaller sized fractions due to the extracting solutions at increased alkaline concentration (Hamdani et al., 2018). This trend agreed with the others performing alkaline-assisted extraction to prepare polysaccharides from other plants sources such as brown seaweed (Nogueira et al., 2022) and mungbean skin (Chen et al., 2022).

3.2. Effect of MNMs prepared using different extracting solutions for composite hydrogel preparation

Then, the MNM_{0M}, $MNM_{0.05\ M}$, and $MNM_{0.1\ M}$ were employed as a co-structuring agent for Alg-based composite hydrogel formation. In the present step, the mixing ratio between Alg and the mucilage was fixed at 3:1. Properties of the beads were characterized as reported in Table 2. Incorporation of the mucilage had no discernible effect on sphericity of the hydrogels, as evidenced by comparable SI between the control beads without added mucilage and the composite beads. Incorporation of konjac glucomannan and xanthan gum as a co-structuring agent led to irregular shape of the composite Alg-based hydrogels (Jing et al., 2025). It should be noted that improvement on spherical uniformity could enhance bioactive compound encapsulation efficiency of the hydrogels by associating with a precise controlled release of the encapsulated compounds (Batisca et al., 2017).

Inclusion of $MNM_{0.05\ M}$ and $MNM_{0.1\ M}$ led to a decrease in hardness of the hydrogels. This behavior might be attributed to intense interaction between Alg and the alkaline extracted MNMs compared to the water extracted gums (MNM_{0M}). It was previously suggested that the interaction between Ca^{2+} and the carboxyl groups of gel structuring agents (polymer-cation-polymer interaction) was stronger than the interaction between the gel structuring agents (polymer-polymer interaction) (Jing et al., 2025; Rezvanian et al., 2017). Incorporation of other polysaccharides involving gum Arabic; κ-carrageenan; low methoxyl pectin; konjac glucomannan; gellan gum; and xanthan gum, also led to lowered hardness of the Alg-based composite hydrogels (Jing et al., 2025). Denser and more rigid network formation of the hydrogel structuring agents might reduce an elastic nature, resulting in a brittle network with lower strength of the gel matrix (Yadav et al., 2021).

Thermal behavior of the hydrogels was determined, and their DSC thermograms are shown (Fig. 2A). For all hydrogel samples, there are a small endothermic peak (marked with the arrows in Fig. 2A) with peak temperature (T_{peak}) of ca. 78–83 °C and two distinctive peaks involving an endothermic peak (peak A) with T_{peak} of ca. 160–165 °C and an exothermic peak (peak B) with T_{peak} of ca. 260 °C. The small endothermic peaks might be attributed to dehydration of the polysaccharides (Nair et al., 2020). The endothermic peak A might relate with melting, whereas the exothermic peak B might associate with degradation of the biopolymers (Flamminii et al., 2020; Rezvanian et al., 2017). These thermal events differ depending on composited monosaccharide moieties and molecular rearrangement of the polysaccharides. The dehydration temperatures of 68.0, 85.3, and 90.1 °C were reported for gum Arabic (Nair et al., 2020), tamarind seed polysaccharide (Harmanmeet et al., 2012), and Senegrain seed polysaccharide (Nairet al., 2020), respectively. The melting temperature (decomposition temperature) of some polysaccharides have been reported, such as 270.8 °C (318.5 °C) for tamarind seed polysaccharide (Harmanmeet et al., 2012) and 184.4 °C (291.3 °C) for carboxymethyl tamarind kernel polysaccharide (Dagar et al., 2023).

Incorporating MNMs affected thermal behavior of the Alg based composite hydrogels, as shown in Table 2. As compared to the control sample, the peak A of the hydrogels added with the MNMs became broader, likely due to overlap of the melting peaks of Alg and the MNMs. Similar behavior was observed for the Alg gel network incorporated with pectin (Rezvanian et al., 2017). Furthermore, amalgamation of Alg and the MNMs led to the hydrogels with increased enthalpy of the peak A suggesting improved thermal stability of the beads. This result might imply cross-linking between the MNMs and Alg, thereby enhancing thermal stability of the hydrogel network (Flamminii et al., 2020; Rezvanian et al., 2017). Notably, there was no significant difference in thermal behavior of the Alg hydrogels added with the MNMs extracted by the NaOH solutions at different concentrations.

Fig. 2B reveals FT-IR profiles of the hydrogels, in which the spectra classically related to the polysaccharides were present as discussed previously (Apoorva et al., 2020; Flamminii et al., 2020). Incorporation of the MNMs, especially for the alkaline-extracted ones, led to alteration in the FT-IR spectra of the hydrogels, which might be attributed due to rearrangement of the hydrocolloids network within the hydrogel matrix (Flamminii et al., 2020). As compared to the control and the Alg+MNM_{0M} beads, increased intensity of the peaks at ca. 1600 and 1030 cm^{-1} was observed for the Alg+$MNM_{0.05\ M}$ and the Alg+$MNM_{0.1\ M}$ hydrogels. Additionally, there was an upward shift of the peaks at ca. 3000–3500 cm^{-1} (representing the –OH groups) for the Alg+$MNM_{0.05\ M}$ and the Alg+$MNM_{0.1\ M}$ compared to the control and the Alg+MNM_{0M} hydrogels. Enhancement on molecular interactions between Alg–pea protein (Qiu et al., 2023); and Alg–pectin (Jing et al., 2025) was also indicated by alteration of the FT-IR peak at ca. 3300 and 3400 cm^{-1}, respectively. The peak at ca. 1030 cm^{-1} of the Alg based gel might relate to a tensile vibration of the ether bond (–O–) on the calcium salt bridge, so increasing on the peak intensity due to the $MNM_{0.05\ M}$ and $MNM_{0.1\ M}$ incorporation might imply strengthening effect of the mucilage to Alg gel structure (Jing et al., 2025).

Morphology of the Alg hydrogels and the ones added with the MNMs were shown in Fig. 3. Improved microstructure of the beads could be observed for the beads of Alg+$MNM_{0.05\ M}$ and Alg+$MNM_{0.1\ M}$ as indicated by their smoother surface and finer inner network formation compared to the control and the Alg+MNM_{0M} beads. The hydrogel with rough surface might allow a penetration of oxygen, acid, bile salts, and digestive enzymes, resulting in degradation of the encapsulated compounds (Jing et al., 2025; Mousavi et al., 2020). Moreover, smooth and continuous inner structure of the gel network closely related to encapsulation and release performance of the hydrogels (Apoorva et al., 2020; Cortez-Trejo et al., 2021; Ćujić et al., 2016). Effect of the MNMs to improve microstructure of the composite gel matrix might be supposed since the enhanced interactions between Alg and the alkaline-extracted MNMs (Apoorva et al., 2020; Flamminii et al., 2020), as well as a filling effect of the mucilage to the pores within Alg gel matrix (Jing et al., 2025). It should be noted that as extracted by the alkaline solutions at increased concentrations, the derived MNMs tended to have greater hydrophilicity as previously implied by the higher solubility (Table 1)

Table 2
Characteristic of the hydrogels prepared using Alg and MNMs prepared by different extracting solutions.

Structuring agents	SI ^{ns}	Hardness (g)	Thermal behavior					
			Peak A (endothermic peak)			Peak B (exothermic peak)		
			T_{onset} (°C)	T_{peak} °C)	enthalpy (J/g)	T_{onset} (°C)	T_{peak} (°C)	enthalpy (J/g)
Alg (control)	1.24 ± 0.08	35.59v2.01^{a}	165.09 ± 4.00	166.17 ± 1.32	257.08 ± 8.23^{b}	231.34 ± 3.01	263.50 ± 1.51	182.39 ± 6.15
Alg+MNM_{0M}	1.30 ± 0.10	38.21 ± 3.11^{a}	161.64 ± 2.50	163.50 ± 4.11	303.40 ± 10.21^{a}	226.13 ± 5.12	263.50 ± 0.74	193.99 ± 11.22
Alg+$MNM_{0.05M}$	1.35 ± 0.12	28.73 ± 1.02^{b}	163.27 ± 1.75	165.33 ± 0.90	282.53 ± 12.19^{a}	234.66 ± 2.66	262.50 ± 2.35	185.44 ± 7.01
Alg+$MNM_{0.1M}$	1.25 ± 0.06	25.62 ± 3.05^{b}	162.49 ± 3.05	164.50 ± 2.11	288.68 ± 8.19^{a}	236.91 ± 4.31	263.17 ± 0.55	180.83 ± 13.01

In each column, different superscripts indicate difference between the means ($p \leq 0.05$).

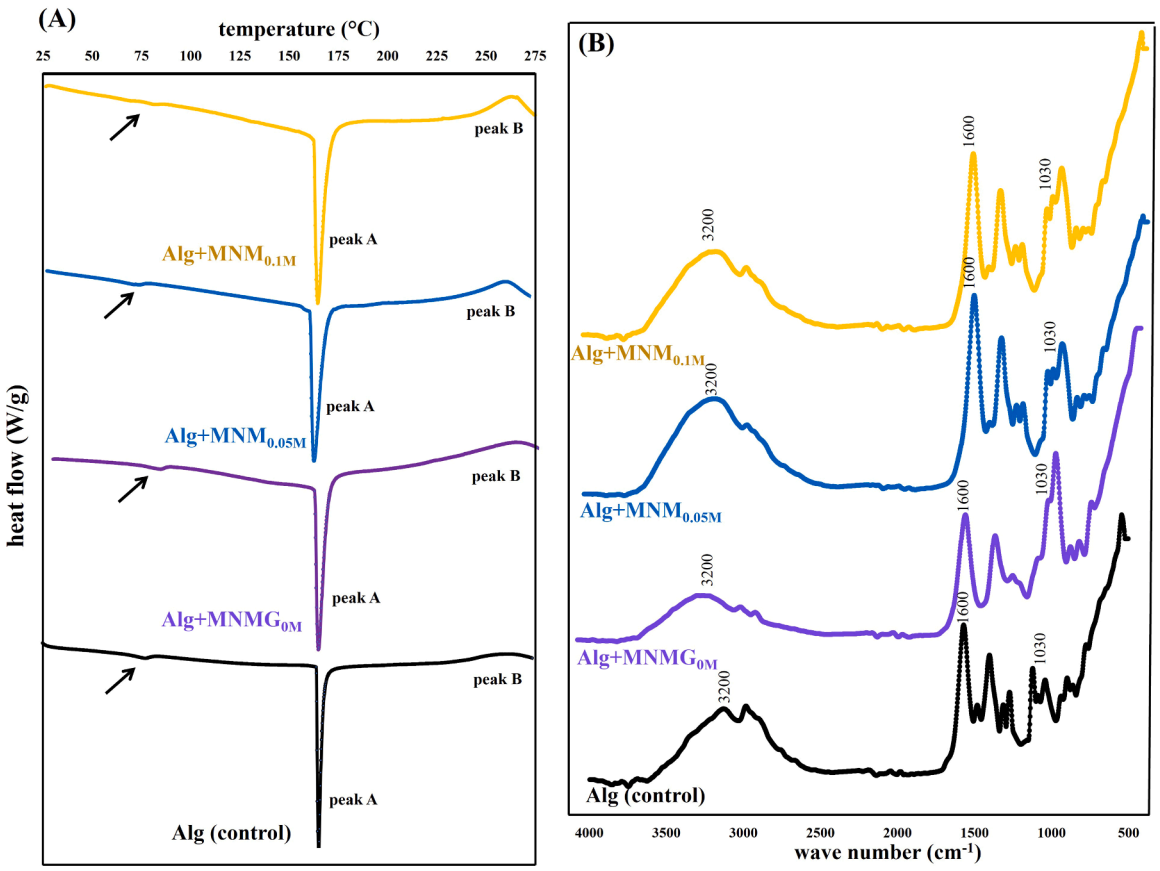

Fig. 2. **(A)** DSC thermograms and **(B)** FT-IR profiles of the composite hydrogels prepared using Alg and MNMs extracted by different extracting solutions.

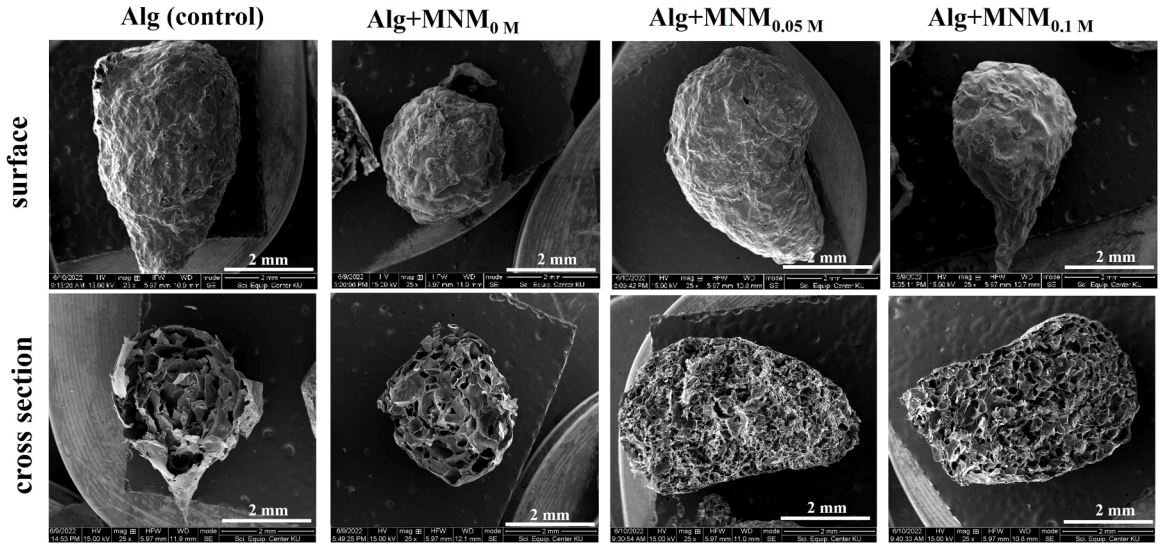

Fig. 3. Morphology of the hydrogels prepared using Alg and MNMs extracted by different extracting solutions.

and the FT-IR spectra with greater exposed monosaccharide moieties (Fig. 1). Therefore, interaction of Alg and the MNMs extracted by the alkaline solutions at increased concentration might be supposed through a preferable hydrogen– and glycosidic bond formation within the hydrocolloids network (Apoorva et al., 2020; Flamminii et al., 2020; Qiu et al., 2023). This effect might explain the improved heat stability of the beads prepared using $MNM_{0.05\ M}$ and $MNM_{0.1\ M}$ (Table 2). Superior gelling ability was also reported for the alkaline-extracted MNMs compared to the counterparts prepared using water extraction (Srichamroen & Chavasit, 2011b).

One of the limitations of Alg-based hydrogels used for encapsulating bioactive compounds was their limited encapsulation capacity due to a formation of gel network with high porosity (Jing et al., 2025; Mirmazloum et al., 2021; Neuenfeldt et al., 2021). By using a co-structuring agent, improvement in capability of the Alg hydrogels to entrap phenolic rich extracts from some plant sources has been reported, such as olive leaves (Flamminii et al., 2020), brewer spent grain (Nuchchareonpaiboon and Prabsangob, 2023), and Chokeberry (Ćujić

et al., 2016), resulting in the enhanced bioactivities of the encapsulated compounds. Microstructure with smooth surface and continuous internal network is always associated with efficiency of the gel matrix in encapsulating bioactive compounds with a good control release (Apoorva et al., 2020; Cortez-Trejo et al., 2021; Jing et al., 2025; Mousavi et al., 2020). Therefore, the present results suggest that $MNM_{0.05\ M}$ and $MNM_{0.1\ M}$ might be appropriately used as a co-structuring agent to improve encapsulation efficiency of Alg hydrogels. Given the comparable extractable yield and lower amount of the alkaline used, the $MNM_{0.05\ M}$ was selected as the representative for further study.

3.3. *Effects of Alg:$MNM_{0.05\ m}$ ratio on property of the composite hydrogel*

Next, effect of mixing ratio of the co-structuring agents on properties of the composite hydrogels were examined. The amount of the selected mucilage–i.e., $MNM_{0.05\ M}$– was increased from a former part, owing to health promoting effect of the mucilage (Phlicharoenphon et al., 2018; Srichamroen & Chavasit, 2011a, b). The composite hydrogels were prepared at varying Alg:$MNM_{0.05\ M}$ weight ratios–i.e., 3:1, 2:1, and 1:1–and then characterized (Table 3). Increasing $MNM_{0.05\ M}$ content could enhance Alg bead formability as suggested by a reduction of SI for the beads with increased $MNM_{0.05\ M}$ content. Using inulin as a co-structuring agent also led to improved Alg hydrogel formability (Ćujić et al., 2016). Difference on hardness of the hydrogels with varying $MNM_{0.05\ M}$ content was not presently observed. However, enthalpy of the endothermic peaks of the hydrogels decreased with increased $MNM_{0.05\ M}$ content. This behavior might be due to lower enthalpy of the $MNM_{0.05\ M}$ (approximately 220 J/g) as compared to Alg (approximately 270 J/g) (*data not shown*).

Fig. 4A depicts FT-IR profile and microstructure of the hydrogels prepared at varying Alg:$MNM_{0.05\ M}$ ratios. The typical peaks associated with the Alg hydrogels prepared using alkaline-extracted MNMs (Fig. 2B) were observed for all the hydrogels. Increase the $MNM_{0.05\ M}$ content led to increment intensity of the peaks at ca. 1410 cm^{-1}; and 1030 cm^{-1} relating to bending of C–H; and the vibration of C–O–C and C–O–H bonds, respectively. This behavior might occur due to preferable interactions between the hydrogel structuring agents through hydrogen and glycosidic bonding, owing to the presence of –OH and –COOH groups of the $MNM_{0.05\ M}$, especially at increased concentration (Apoorva et al., 2020; Flamminii et al., 2020; Qiu et al., 2023). Enhancement of intermolecular interactions between Alg and $MNM_{0.05\ M}$ at increased content was also supported by microstructure of the beads (Fig. 4B): The beads with smoother surface and denser gel network tended to be found for the beads prepared at increased content of the $MNM_{0.05\ M}$, implying a filling effect of the $MNM_{0.05\ M}$ to reinforce Alg gel matrix formation. This trend aligns with the previous reports studying on characteristics of the composite hydrogels prepared using Alg together with inulin (Ćujić et al., 2016); pectin (Flamminii et al., 2020); and tragacanth gum (Apoorva et al., 2020) as a co-structuring agent.

To assess stability of the beads, ΔSI of the hydrogels as affected by heating and storage in different pH environments was estimated (Fig. 5). Lower ΔSI indicates better stability with lesser degree of bead swelling and always associates with better controlled release of the bioactive compounds encapsulated in the hydrogel matrix (Apoorva et al., 2020; Jing et al., 2025). Presently, the hydrogels demonstrated superior stability in the acidic pH condition as compared to neutral pH, as indicated by the lowest ΔSI of the beads kept at pH 3.0. This trend was consistent with others (Camacho et al., 2019; Nuchchareonpaiboon & Prabsangob, 2023) and might be ascribed to different interaction affinity of the biopolymers in dissimilar pH environments. Guluronic and mannuronic acids, the major monomer block of Alg, possess pKa at pH 3.2 and 4.0, respectively (Camacho et al., 2019). In the acidic condition with pH lower than their pKa, carboxylic groups of guluronic and mannuronic acids were present as COOH, so intermolecular interactions of the biopolymers could be enhanced via hydrogen bonding, resulting in a strengthen hydrogel structure (Qiu et al., 2023). In the neutral condition with pH higher than their pKa, on the other hand, the carboxylic groups of guluronic and mannuronic acids are available as COO^-, leading to a relaxation in intermolecular interaction between Alg molecules due to a repulsive force of the negative charges, resulting in bead swelling (Camacho et al., 2019).

Interestingly, incorporation of the $MNM_{0.05\ M}$ at sufficient levels, specifically at mixing ratios of 2:1 and 1:1, significantly improved stability of the hydrogels against storage at all observed pH conditions. The improved stability of the Alg-$MNM_{0.05\ M}$ beads might be expected since the microstructure with smoother surface and more continuous internal network of the hydrogels prepared using the $MNM_{0.05\ M}$, particularly at the increased mucilage content as previously observed in Fig. 4B (Jing et al., 2025). Robust chemical interactions between the hydrocolloids could hinder water permeable, thereby lowering swelling degree of the composite hydrogels (Lin et al., 2021; Tiamiyu et al., 2023). Lowered swelling degree of the composite hydrogels prepared using the $MNM_{0.05\ M}$ at increased content might suggest effective encapsulation efficiency of the beads (Jing et al., 2025). Although incorporation of gum Arabic affected to diminish swelling of the Alg-based gel stored at the acidic condition of pH 2.0, greater swelling of the Alg-gum Arabic composite hydrogels compared to the Alg hydrogels was observed at the neutral condition of pH 7.0 (Jing et al., 2025). Interestingly, adding $MNM_{0.05\ M}$ led to lowered swelling degree of the composite beads as compared to the Alg-based hydrogels without the mucilage in both acidic and neutral conditions. The present results might imply capability of the Alg-$MNM_{0.05\ M}$ composite hydrogels to protect the encapsulated compounds from acid, bile salts, and digestive enzymes in the gastrointestinal tract of human effectively.

Regarding effect of heating, there was a positive relationship between ΔSI and the duration of heating, suggesting the influence of heating on bead swelling. However, when the beads were prepared using Alg:$MNM_{0.05\ M}$ at the ratios of 2:1 and 1:1, they displayed improved stability against heating. Incorporation of $MNM_{0.05\ M}$ at sufficient level could enhance Alg hydrogel stability which might be attributed to a tight gel network formation between Alg and $MNM_{0.05\ M}$, especially at increased $MNM_{0.05\ M}$ content, thereby restricting bead swelling (Apoorva et al., 2020; Jing et al., 2025). This result was concurrent with the FT-IR profile and microstructure of the beads as previously shown (Fig. 4). Development of heat stability of the Alg hydrogels could be also achieved by employing low methoxyl pectin and

Table 3
Characteristic of the hydrogels prepared using Alg and $MNM_{0.05\ M}$ at different weight ratios.

Alg:$MNM_{0.05M}$	SI	hardness (g)	thermal behavior					
			peak A (endothermic peak)			peak B (exothermic peak)		
			T_{onset} (°C)	T_{peak} (°C)	enthalpy (J/g)	T_{onset} (°C)	T_{peak} (°C)	enthalpy (J/g)
3:1	1.31 ± 0.12^{a}	27.93 ± 0.82	163.12 ± 4.56	166.00 ± 2.05	298.80 ± 10.01^{a}	228.63 ± 3.05	264.10 ± 4.00	193.19 ± 12.32
2:1	1.13 ± 0.06^{ab}	27.00 ± 1.20	166.76 ± 1.21	168.83 ± 1.75	290.11 ± 12.19^{ab}	229.60 ± 1.55	262.50 ± 3.05	192.44 ± 7.01
1:1	1.00 ± 0.07^{b}	26.55 ± 2.21	164.26 ± 2.00	165.67 ± 3.11	257.01 ± 8.19^{c}	230.91 ± 2.75	262.70 ± 2.57	198.83 ± 9.31

In each column, different superscripts indicate difference between the means ($p \leq 0.05$).

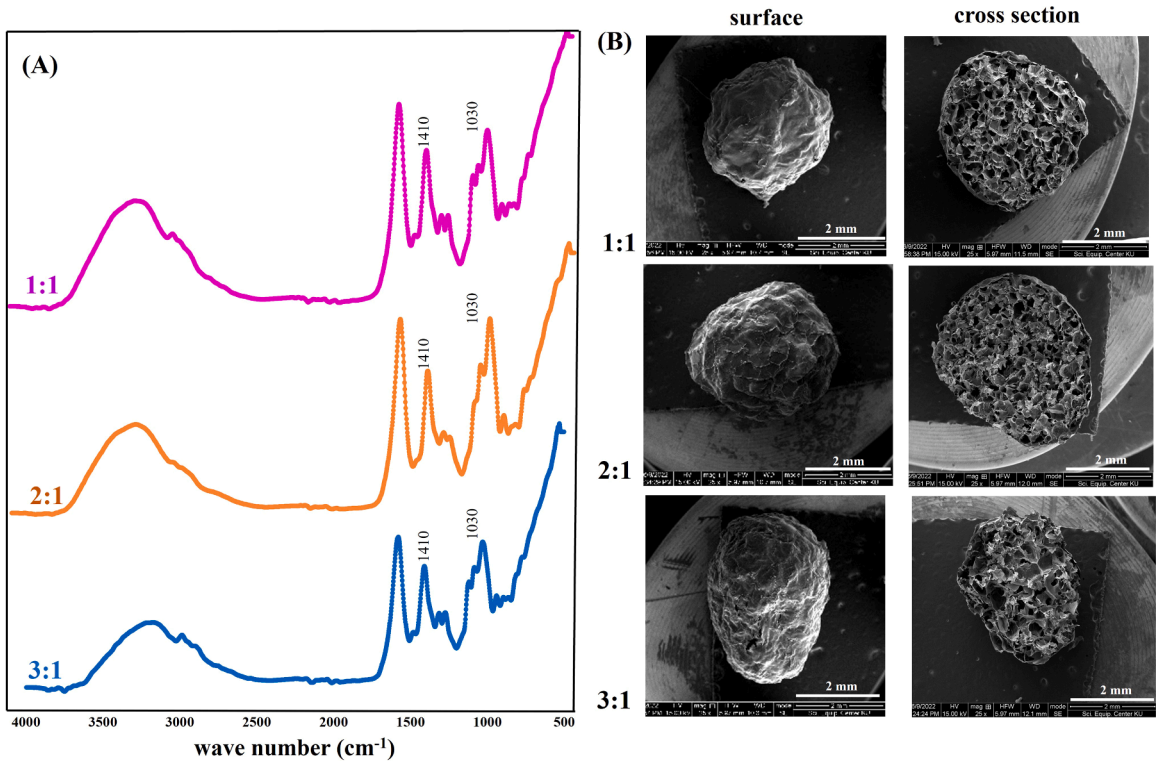

Fig. 4. **(A)** FT-IR profiles and **(B)** morphology of the hydrogels prepared using Alg:$MNM_{0.05\ M}$ at different ratios.

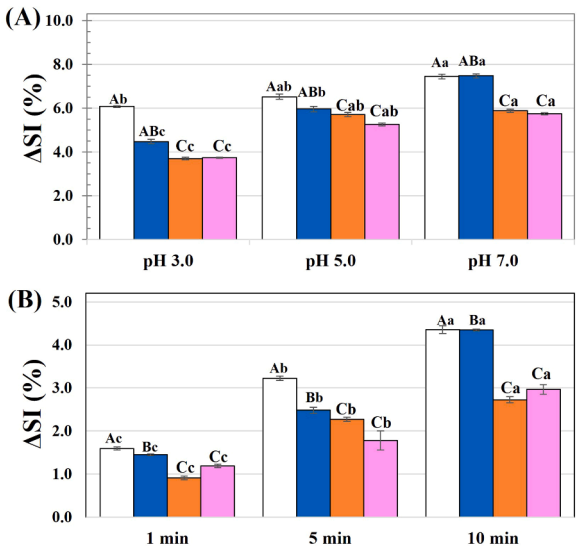

Fig. 5. Effects of **(A)** storage pH and **(B)** heating time on ΔSI of the hydrogels prepared using Alg:$MVG_{0.05\ M}$ at different ratios including 1:0 (control, □), 3:1 (■), 2:1 (■), and 1:1 (■). In each subfigure, different capital letters indicate difference between means as affected by Alg:$MNM_{0.05\ M}$ ratio ($p \leq 0.05$). Different small letters indicate difference between means as affected by storage pH condition (Fig. 5A) and heating time (Fig. 5B) ($p \leq 0.05$).

κ-carageenan (Jing et al., 2025) as a co-structuring agent, resulting in the improved viability of the encapsulated probiotic microorganism.

For the next study, the hydrogels prepared using Alg:$MNM_{0.05\ M}$ at the ratio of 2:1 were selected due to their good stability without significant effect on thermal behavior of the hydrogels.

3.4. The composite hydrogels for RE encapsulation

The composite hydrogels prepared using Alg:$MNM_{0.05\ M}$ at the ratio of 2:1 were prepared by loading RE at different concentrations (1, 2.5, and 5 %): The beads incorporated with RE at were labeled as RE-1, RE-2.5, and RE-5, respectively. Then, characteristics of the RE loaded hydrogels were examined (Table 4). There was no significant difference in SI of the beads incorporated with RE at varying concentrations. However, the hardness of RE-2.5 and RE-5 was significantly lower than RE-1. A positive correlation between LE and added RE content was observed, and increasing RE concentration to 2.5 % led to an improved EE of the beads to approximately 60 %. Comparable EE (ca. 62–78 %) has been reported for the Alg hydrogels used for phenolic extract encapsulation when tragacanth gum was employed as a co-structuring agent (Apoorva et al., 2020). Molecular characteristics of the hydrocolloids employed as a co-structuring agent crucially affected encapsulation effectiveness of the hydrogels. With hydrophilic nature, the extracted gum might interact preferably with Alg and/or the bioactive compounds present in RE, resulting in enable efficiency for phenolic loading and encapsulation capacity of the hydrogels (Balanč et al., 2016; Belščak-Cvitanovic et al., 2016; Ćujić et al., 2016). Phenolic entrapability of the Alg hydrogels could be also improved by employing inulin with hydrophilicity as a co-structuring agent, which was described to a preferably binding affinity of inulin with phenolic compounds (Ćujić et al., 2016). Considering thermal properties of the hydrogels loaded with RE, there was an increase in enthalpy of the endothermic peak A for the RE-5, indicating improved thermal stability of the beads, possibly due to the enhanced intermolecular interactions among the compounds in the hydrogel matrix (Flamminii et al., 2020).

Characteristics of the hydrogels were further examined by observing FT-IR spectra and microstructure of the beads (Fig. 6). Loading of RE affected FT-IR spectra of the hydrogels: There was an emergence of new peaks and intensity increase for the existing peaks relating to phenolic compounds. These peaks included those at ca. 1015 cm^{-1} signifying a stretching vibration of C–O; the peaks at ca. 1325 cm^{-1} representing

Table 4
Characteristic of Alg-$MNM_{0.05\ M}$ hydrogels loaded with RE at different concentrations.

Hydrogels	SI	Hardness (g)	LE (mgGAE/g, db)	EE (%)	Thermal behavior					
					peak A (endothermic peak)			peak B (exothermic peak)		
					T_{onset} (v)	T_{peak} (v)	enthalpy (J/g)	T_{onset} (°C)	T_{peak} (°C)	enthalpy (J/g)
RE-1	1.07 ± 0.06	26.56 ± 2.12[a]	1.15 ± 0.44[c]	55.56 ± 0.82[b]	197.12 ± 4.05[a]	198.33 ± 2.05[a]	272.13 ± 3.55[b]	235.50 ± 3.05	263.50 ± 3.00	202.33 ± 8.31
RE-2.5	1.06 ± 0.06	21.39 ± 0.73[b]	2.62 ± 0.14[b]	60.32 ± 1.07[a]	200.01 ± 1.05[a]	201.33 ± 3.57[a]	277.73 ± 7.06[b]	236.00 ± 2.75	265.00 ± 1.05	197.78 ± 12.31
RE-5	1.07 ± 0.07	21.52 ± 0.71[b]	5.28 ± 0.28[a]	61.33 ± 0.89[a]	174.14 ± 3.55[b]	174.83 ± 5.66[b]	305.19 ± 5.11[a]	238.50 ± 2.55	267.25 ± 2.55	198.85 ± 7.22

In each column, different superscripts indicate difference between the means ($p \leq 0.05$).

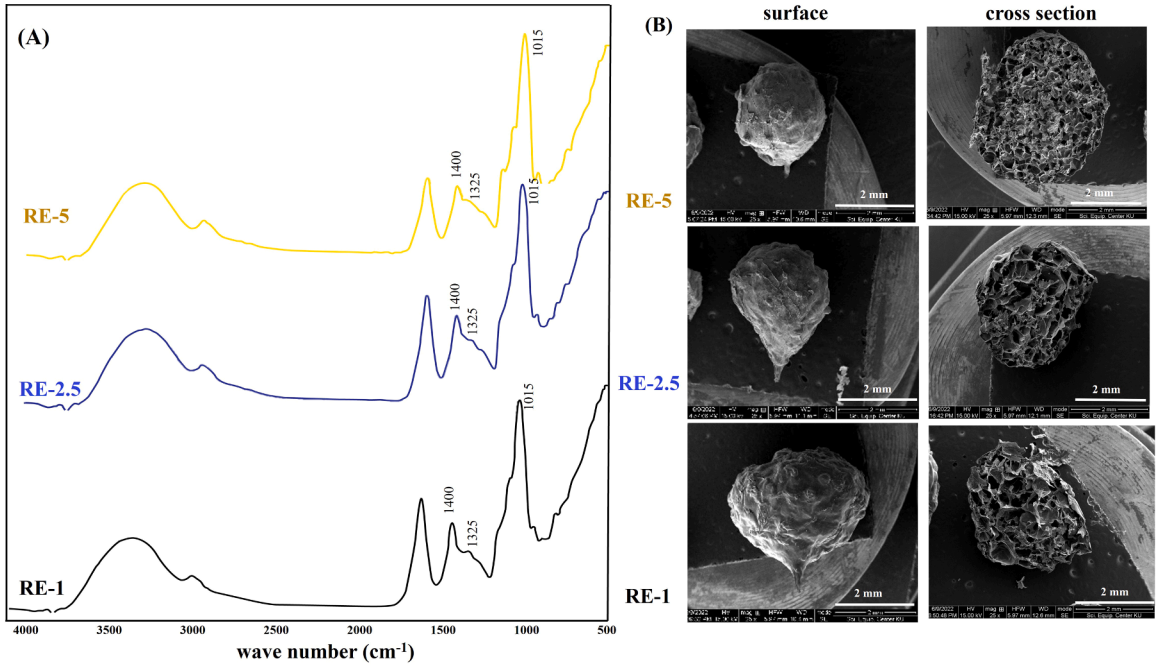

Fig. 6. **(A)** FT-IR profiles and **(B)** morphology of the Alg-$MNM_{0.05\ M}$ composite hydrogels loaded with RE at different concentrations.

–CH bending and wagging of CH_2; and the peaks at ca. 1400 cm^{-1} implying symmetric in-plane bending of CH_3 (Silva et al., 2014). Shift in the FT-IR peak at ca. 3000 cm^{-1} was observed for the hydrogels added with RE at increased concentration, corresponding with the integration of the essential oils into the Alg-based coacervates (Qiu et al., 2023). These results suggested a successful RE incorporation into the Alg-$MNM_{0.05cM}$ composite gel matrix. Interestingly, the beads showed improved microstructure with smoother surface and denser gel network with the presence of RE, especially at the increased RE content. This effect might occur due to preferable interaction between the hydrogel structuring agents and the chemical composition of RE as implied by the FT-IR spectra (Fig. 6A). Similar behavior was also found for the hydrogel added with *Lamiaceae* plant phenolic extract (Benković et al., 2021).

3.5. Stability and in vitro phenolic compound releasing of the composite hydrogels

Stability of the composite hydrogels loaded with RE was evaluated after storing them in different pH conditions and subjecting them to various heating times (Fig. 7). After one week of storage, the highest phenolic loss was observed in the beads stored at pH 7.0, aligning with the highest reduction in the free radical scavenging ability of the beads. The lower stability at neutral pH compared to acidic environment was previously suggested (Fig. 5A). Higher degree of swelling is always associated with a lower encapsulation capability of hydrogels (Jing et al., 2025). Regarding effect of heating, prolonged heating time for 10 min resulted in a significant phenolic loss which was consistent with considerable decrease in DPPH radical scavenging capability of the beads after 10 min of heating. However, incorporating RE at higher concentration tended to improve phenolic sustainability of the beads against both storage in different pH conditions and longer heating times: Lowered ΔTPC and ΔDPPH free radical scavenging ability were observed for RE-2.5 and RE-5 as compared to RE-1. This trend might suggest the availability of the bioactive compounds in the beads loaded with higher RE concentration.

Phenolic releasing behavior of the hydrogels was further examined through an *in vitro* gastric and intestinal model (Fig. 7E). Almost no phenolic release was observed during the simulated gastric phase implying good stability of the hydrogels in a harsh acidic condition of the stomach environment. During the intestinal phase, phenolic release increased gradually over the entire digestion time. This trend was correlated with the Alg-tragacanth gum hydrogels loaded with phenolic extract (Apoorva et al., 2020) and folic acid (Camacho et al., 2019). Effective phenolic compound retaining of the hydrogels in the stomach phase might be relevant to their less swelling (Fig. 5A) and greater phenolic retention (Fig. 7A) in the acidic environment. On the other hand, greater phenolic release in the intestinal phase correlated with higher swelling and reduced phenolic retention of the hydrogels

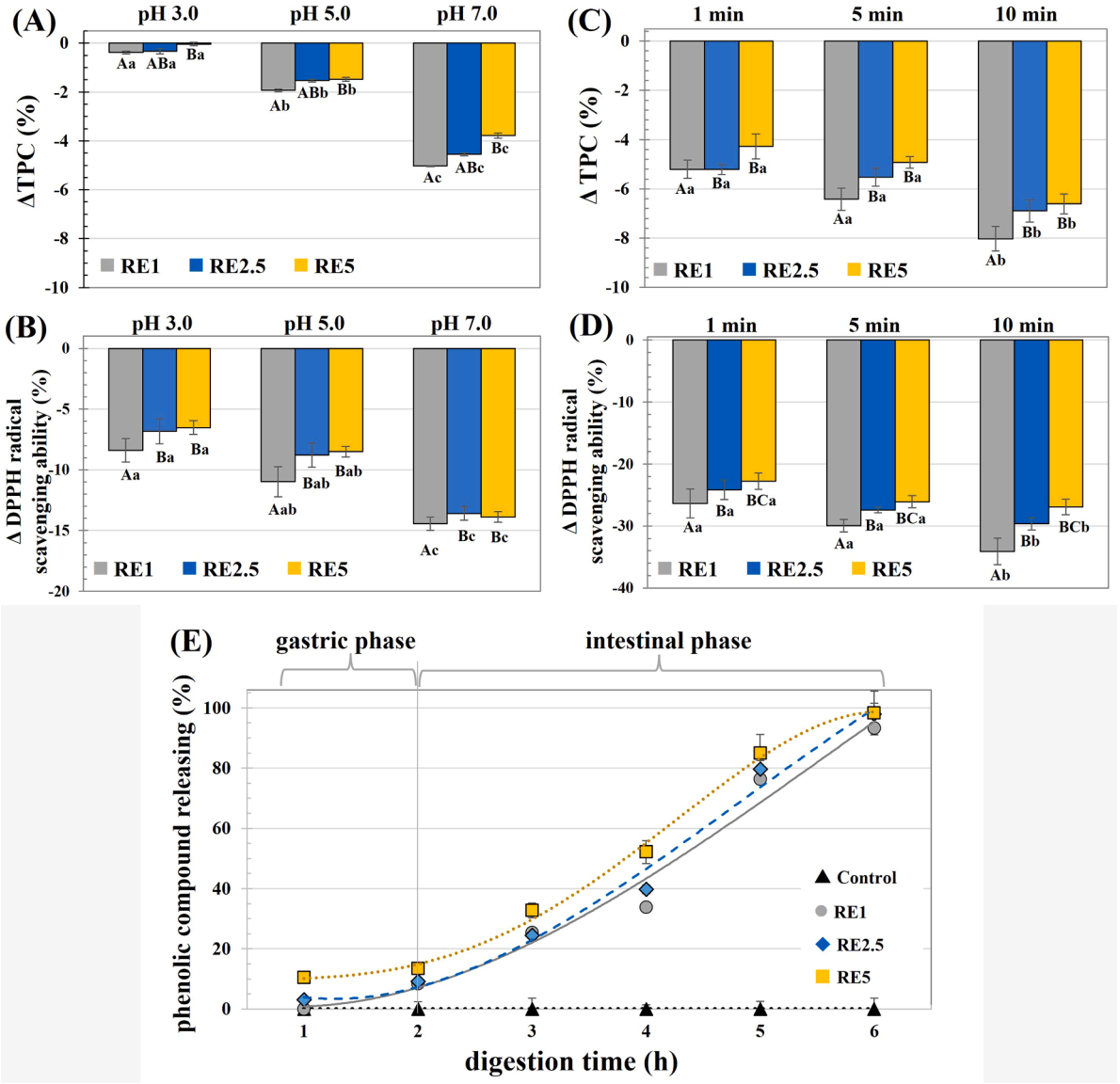

Fig. 7. Characteristics of the hydrogels loaded with RE at different concentrations as affected by different factors: **(A and B)** storage pH stability, **(C and D)** heating stability, and **(E)** phenolic releasing observed *in vitro* simulated gastric and intestinal phases. In subfigures **A** to **D**, different capital letters indicate difference between means as affected by RE content ($p \leq 0.05$). Different small letters indicate difference between means as affected by storage pH condition (Fig. 7A and B) and heating time (Fig. 7C and D) ($p \leq 0.05$).

observed at the neutral pH conditions. Swelling of the beads was a crucial factor governing the release of bioactive compounds from the gel matrix, in which release of bioactive compounds occurred with bead swelling and subsequent degradation of the hydrogel structure (Lin et al., 2021). Importantly, there was no difference in the phenolic release behavior of the beads containing RE at different concentrations, indicating the efficiency of the composite hydrogels in retaining bioactive compounds. Improvement in phenolic entrapability of the Alg hydrogels was also reported when starch and pectin were used as a co-structuring agent (Dadwal et al., 2021). The interaction between the hydrogel structuring agents and the components of RE as implied by the FT-IR profile (Fig. 6A) might reduce the release of bioactive compounds from the hydrogel matrix, allowing effective TPC retainability of the beads (Apoorva et al., 2020). Enhanced interaction between the hydrogel structuring agents and bioactive compounds could lead to higher loading efficiency of the microbeads (Belščak-Cvitanovic et al., 2016; Ćujić et al., 2016; Lin et al., 2021). It's worth noting that the MNM consisted of dietary fibers with limited digestibility in the mammal GI tract (Srichamroen & Chavasit, 2011a), so lowering in releasing of encapsulated bioactive compounds might be expected for the hydrogels incorporated with the MNM (Apoorva et al., 2020). Appropriate release characteristics of the hydrogels may enhance the absorption and bioavailability of phenolic compounds. In this study, most phenolic compounds were released from the beads at the end of intestinal phase, thereby suggesting potential of the Alg-$MNM_{0.05\ M}$ hydrogels as a bioactive compound carrier system. However, studying on the bioactive compound releasing behavior of the fabricated hydrogels in both kinetic mechanism and interaction with other food components should be further performed for better control release of the encapsulated compounds.

4. Conclusions

The MNMs possessed a promising role as a co-structuring agent to enhance stability and encapsulation efficiency of the composite Alg-based hydrogels. Alkaline aided extraction significantly improved MNM capability to strengthen the Alg hydrogel matrix as evidenced by the improved microstructure of the beads. Presently, the mucilage

extracted by 0.05 M NaOH ($MNM_{0.05\ M}$) was selected as a representative. Employing $MNM_{0.05\ M}$ as a co-structuring agent led to the composite hydrogels with improved microstructure and stability against heating and storage at varying pH conditions, likely due to preferably intermolecular interactions between Alg and the mucilage. Subsequently, Alg-$MNM_{0.05\ M}$ composite hydrogels were employed to encapsulate RE, where the interaction between the hydrogel structuring agents and the chemical composition of RE led to enhanced stability and phenolic retainability of the beads. Notably, the fabricated composite hydrogels loaded with antioxidative RE exhibited stability in the simulated stomach environment and primarily released phenolic compounds during the simulated intestinal phase. This study suggested the potential of MNM to enhance stability and encapsulation efficiency of the composite Alg-based hydrogels. Moreover, owing to health promoting effect of the MNM, the elaborated hydrogels might feasibly role as a functional ingredient for development of functional foods thereafter.

Data Availability

Data is contained within the article and available on request from the corresponding author.

Ethical statement

"The research presented does not involve any animal or human study".

CRediT authorship contribution statement

Nopparat Prabsangob: Writing – original draft, Visualization, Project administration, Methodology, Funding acquisition, Conceptualization. **Sasithorn Hangsalad:** Formal analysis. **Utai Klinkesorn:** Writing – review & editing. **Tan Chin Ping:** Writing – review & editing.

Declaration of competing interest

Authors declare to not have conflict of interest for this paper publishing.

Acknowledgment

This work was supported by the Kasetsart University Research and Development Institute (KURDI) under the project Development of Advance Researcher Competence System for Competitiveness in Agriculture and Food, grant number FF(KU) 25.64.

References

Ahmad, R., Riaz, M., Khan, A., Ajjamea, A., Algheryafi, M., Sewaket, D., & Alqathama, A. (2021). *Ganoderma lucidum* (Reishi) an edible mushroom; A comprehensive and critical review of its nutritional, cosmeceutical, mycochemical, pharmacological, clinical, and toxicological properties. *Phytotherapy Research, 35*, 6030–6062. https://doi.org/10.1002/ptr.7215

Alex, L. C., Lorena, D., & Miriam, M. (2013). Effect of starch filler on calcium-alginate hydrogels loaded with yerba mate antioxidants. *Carbohydrate Polymers, 95*, 315–323. https://doi.org/10.1016/j.carbpol.2013.03.019

Apoorva, A., Rameshbabu, A. P., Dasgupta, S., Dhara, S., & Padmavati, M. (2020). Novel pH-sensitive alginate hydrogel delivery system reinforced with gum tragacanth for intestinal targeting of nutraceuticals. *International Journal of Biological Macromolecules, 147*, 675–687. https://doi.org/10.1016/j.ijbiomac.2020.01.027

AOAC. (1990). Official methods of analysis. *Association of official analytical chemistry*. Airlington.

Balanč, B., Kalušević, A., Drvenica, I., Coelho, M. T., Djordjević, V., Alves, V. D., Sousa, I., Moldao-Martins, M., Rakić, V., Nedović, V., & Bugarski, B. (2016). Calcium-alginate-inulin microbeads as carrier for aqueous Carqueja extract. *Journal of Food Science, 81*, 65–75. https://doi.org/10.1111/1750-3841.13167

Batisca, D. P. C., Oliveira, I. N., Ribeiro, A. R. B., Fonseca, E. J. S., Santos-Magalhães, N. C., de Sena-Filho, J. G., Teodoro, A. V., Grillo, L. A. M., de Almeidae, R. S., & Dornelas, C. B. (2017). Encapsulation and release of *beauveria bassiana* from alginate-bentonite nanocomposite. *RSC Advances, 7*, 26468–26477. https://doi.org/10.1039/C7RA02185B

Belščak-Cvitanovic, A., Bušić, A., Barišić, L., Vrsaljko, D., Karlović, S., Špoljarić, I., Vojvodić, A., Mršić, G., & Komes, D. (2016). Emulsion templated microencapsulation of dandelion (*Taraxacum officinale* L.) polyphenols and β-carotene by ionotropic gelation of alginate and pectin. *Food Hydrocolloids, 57*, 139–152. https://doi.org/10.1016/j.foodhyd.2016.01.020

Benković, M., Sarić, I., Tušek, A. J., Jurina, T., Kljusurić, J. G., & Valinger, D. (2021). Analysis of the adsorption and release process of bioactives from *Lamiaceae* plant extracts on alginate microbeads. *Food and Bioprocess Technology, 14*, 1216–1230. https://doi.org/10.1007/s11947-021-02632-z

Brand-Williams, W., Cuvelier, M. E., & Berset, C. (1995). Use of free radical method to evaluate antioxidant activity. *LWT-Food Science and Technology, 28*, 25–30. https://doi.org/10.1016/S0023-6438(95)80008-5

Cai, Y., Qin, W., Ketnewa, S., & Ogawa, Y. (2020). Impact of particle size of pulverized citrus peel tissue on changes in antioxidant properties of digested fluids during simulated *in vitro* digestion. *Food Science and Human Wellness, 9*, 58–63. https://doi.org/10.1016/j.fshw.2019.12.008

Camacho, D. H., Uy, S. J. Y., Cabrera, M. J. F., Lobregas, M. O. S., & Fajardo, T. J. M. C (2019). Encapsulation of folic acid in copper-alginate hydrogels and it's slow *in vitro* release in physiological pH condition. *Food Research International, 119*, 15–22. https://doi.org/10.1016/j.foodres.2019.01.053

Chan, E. S., Lee, B. B., Ravindra, P., & Poncelet, D. (2009). Prediction models for shape and size of Ca-alginate microbeads produced through extrusion-dripping method. *Journal of Colloid and Interface Science, 338*, 63–72. https://doi.org/10.1016/j.jcis.2009.05.027

Chen, S., Qin, L., Xie, L., Yu, Q., Chen, Y., Chen, T., Lu, H., & Xie, J. (2022). Physicochemical characterization, rheological and antioxidant properties of three alkali-extracted polysaccharides from mung bean skin. *Food Hydrocolloids, 132*, Article 107867. https://doi.org/10.1016/j.foodhyd.2022.107867

Chuensun, T., Chewonarin, T., Laopajon, W., Samakradhamrongthai, R. S., Chaisan, W., & Utama-ang, N. (2024). Evaluation of the phytochemical, bioactive compounds and descriptive sensory of encapsulated lingzhi (*Garnoderma lucidum*) extracts with combined wall materials for masking effect on the perception of off-flavour and bitterness. *Heliyon, 10*, Article e40094. https://doi.org/10.1016/j.heliyon.2024.e40094

Cortez-Trejo, M. C., Gayťan-Martínez, M., Reyes-Vega, M. L., & Mendoza, S. (2021). Protein-gum-based gels: Effect of gum addition on microstructure, rheological properties, and water retention capacity. *Trends in Food Science & Technology, 116*, 303–317. https://doi.org/10.1016/j.tifs.2021.07.030

Ćujić, N., Triković, K., Bugarski, B., Ibrić, S., Pljevljakušić, D., & Šavikin, K. (2016). Chokeberry (*Aronia melanocarpa* L.) extract loaded in alginate and alginate/inulin system. *Industrial Crops and Products, 86*, 120–131. https://doi.org/10.1016/j.indcrop.2016.03.045

Dadwal, V., Joshi, R., & Gupta, M. (2021). Formulation, characterization and *in vitro* digestion of polysaccharide reinforced Ca-alginate microbeads encapsulating *Citrus medica* L. phenolics. *LWT-Food Science and Technology, 152*, Article 112290. https://doi.org/10.1016/j.lwt.2021.112290

Dagar, V., Pahwa, R., & Ahuja, M. (2023). Preparation and characterization of calcium cross-linked carboxymethyl tamarind kernel polysaccharide as release retardant polymer in matrix. *Biointerface Research in Applied Chemistry, 13*, Article 111. https://doi.org/10.33263/BRIAC132.111

Doumèche, B., Küppers, M., Stapf, S., Blümich, B., Hartmeier, W., & Ansorge-Schumacher, M. B. (2004). New approaches to the visualization, quantification and explanation of acid-induced water loss from Ca-alginate hydrogel beads. *Journal of Microencapsulation, 21*, 565–573.

Flamminii, F., Di Mattia, C. D., Nardella, M., Chiarini, M., Valbonetti, L., Neri, L., Dofonzo, G., & Pittia, P. (2020). Structuring alginate beads with different biopolymers for the development of functional ingredients loaded with olive leaves phenolic extract. *Food Hydrocolloids, 108*, Article 105849. https://doi.org/10.1016/j.foodhyd.2020.105849

Hamdani, A. M., Wani, I. A., & Bhat, N. A. (2018). Effect of gamma irradiation on the physicochemical and structural properties of plant seed gums. *International Journal of Biological Macromolecules, 106*, 507–515. https://doi.org/10.1016/j.ijbiomac.2017.08.045

Harmanmeet, K., Shikha, Y., Munish, A., & Neeraj, D. (2012). Synthesis, characterization and evaluation of thiolated tamarind seed polysaccharide as a mucoadhesive polymer. *Carbohydrate Polymers, 90*, 1543–1549. https://doi.org/10.1016/j.carbpol.2012.07.028

Hellebois, T., Fortuin, J., Xu, X., Shaplov, A. S., Gaiani, C., & Soukoulis, C. (2021). Structure conformation, physicochemical and rheological properties of flaxseed gums extracted under alkaline and acidic conditions. *International Journal of Biological Macromolecules, 192*, 1217–1230. https://doi.org/10.1016/j.ijbiomac.2021.10.087

Huang, F., Hong, R., Zhang, R., Dong, L., Bai, Y., Liu, L., Jia, X., Wang, G., & Zhang, M. (2019). Dynamic variation in biochemical properties and prebiotic activities of polysaccharides from longan pulp during fermentation process. *International Journal of Biological Macromolecules, 132*, 915–921. https://doi.org/10.1016/j.ijbiomac.2019.04.032

Jing, Y. Y., Li, Y. C., Luo, Y. Q., Zou, L. H., Tang, Y. M., Lin, Y. X., & Meng, F. B. (2025). Effects of gum incorporation on the properties of sodium alginate-based composite hydrogel beads for encapsulating lactic acid bacteria. *Carbohydrate Polymers, 369*, Article 124298. https://doi.org/10.1016/j.carbpol.2025.124298

Kurkuri, M. D., & Aminabhavi, T. M. (2004). Polyvinyl alcohol and polyacrylic acid sequential interpenetrating network pH-sensitive microspheres for the delivery of diclofenac sodium to intestine. *Journal of Controlled Release, 96*, 9–20. https://doi.org/10.1016/j.jconrel.2003.12.025

Le, H. D., Loveday, S. M., Singh, H., & Sarkar, A. (2020). Gastrointestinal digestion of Pickering emulsions stabilized by hydrophobically modified cellulose nanocrystals: Release of short-chain fatty acids. *Food Chemistry, 320*, Article 126650. https://doi.org/10.1016/j.foodchem.2020.126650

Li, Q., Duan, M., Hou, D., Chen, X., Shi, J., & Zhou, W. (2021). Fabrication and characterization of Ca (II)-alginate-based beads combined with different polysaccharides as vehicles for delivery, release and storage of tea polyphenol. *Food Hydrocolloids, 112*, Article 106274. https://doi.org/10.1016/j.foodhyd.2020.106274

Li, Y., Liang, M., Dou, X., Feng, C., Pang, J., Cheng, X., Liu, H., Liu, T., Wang, Y., & Chen, X. (2019). Development of alginate hydrogel/gum Arabic/gelatin based composite capsules and their application as oral delivery carriers for antioxidant. *International Journal of Biological Macromolecules, 132*, 1090–1097. https://doi.org/10.1016/j.ijbiomac.2019.03.103

Lin, D., Kelly, A. L., Maidannyk, V., & Miao, S. (2021). Effect of structuring emulsion gels by whey or soy protein isolate on the structure, mechanical properties, and *in vitro* digestion of alginate-based emulsion gel beads. *Food Hydrocolloids, 110*, Article 106165. https://doi.org/10.1016/j.foodhyd.2020.106165

Lopez-Torrez, L., Nigen, M., Williams, P., Doco, T., & Sanchez, C. (2015). *Acacia senegal* vs. *Acacia seyal* gums—Part 1: Composition and structure of hyperbranched plant exudates. *Food Hydrocolloids, 51*, 41–53. https://doi.org/10.1016/j.foodhyd.2015.04.019

Martín, C. M., López, O. V., Ciolino, A. E., Morata, V. I., Villar, M. A., & Ninago, M. D. (2019). Immobilization of enological pectinase in calcium alginate hydrogels: A potential biocatalyst for winemaking. *Biocatalysis and Agricultural Biotechnology, 18*, Article 101091. https://doi.org/10.1016/j.bcab.2019.101091

Mirmazloum, I., Ladányi, M., Omran, M., Papp, V., Ronkainen, V. P., Pónya, Z., Papp, I., Némedi, E., & Kiss, A. (2021). Co-encapsulation of probiotic *Lactobacillus acidophillus* and Reishi medicinal mushroom (*Ganoderma lingzhi*) extract in moist calcium alginate beads. *International Journal of Biological Macromolecules, 192*, 461–470. https://doi.org/10.1016/j.ijbiomac.2021.09.177

Mousavi, S. M. R., Rafe, A., & Yeganehzad, S. (2020). Structure-rheology relationships of composite gels: Alginate and basil seed gum/guar gum. *Carbohydrate Polymers, 232*, Article 115809. https://doi.org/10.1016/j.carbpol.2019.115809

Nair, R. M., Bindhu, B., & Reena, V. L. (2020). A polymer blend from gum Arabic and sodium alginate–preparation and characterization. *Journal of Polymer Research, 27*, 154. https://doi.org/10.1007/s10965-020-02128-y

Nep, E. I., & Conway, B. R. (2011). Physicochemical characterization of Grewia polysaccharide gum: Effect of drying method. *Carbohydrate Polymers, 84*, 446–453. https://doi.org/10.1016/j.carbpol.2010.12.005

Neuenfeldt, N. H., de Moraes, D. P., de Deus, C., Barcia, M. T., & de Manezes, C. R. (2021). Blueberry phenolic composition and improved stability by microencapsulation. *Food and Bioprocess Technology, 15*, 750–767. https://doi.org/10.1007/s11947-021-02749-1

Nogueira, M. T., Chica, L. R., Yamashita, C., Nunes, N. S. S., Moraes, I. C. F., Branco, C. C. Z., & Branco, I. G. (2022). Optimal conditions for alkaline treatment of alginate extraction from the brown seaweed *sargassum cymosum* C. Agardh by response surface methodology. *Applied Food Research, 2*, Article 100141. https://doi.org/10.1016/j.afres.2022.100141

Nuchchareonpaiboon, P., & Prabsangob, N. (2023). Alginate and malva nut gum-based hydrogels loaded with brewer's spent grain as a source of fiber and antioxidants. *International of Food Research Journal, 30*, 536–547. https://doi.org/10.47836/ifrj.30.2.22

Paulo, F., & Santos, L. (2020). New insights in the *in vitro* release of phenolic antioxidants: The case study of the release behavior of tyrosol from tyrosol-loaded ethylcellulose microparticles during the *in vitro* gastrointestinal digestion. *Colloids Surfaces B: Biointerfaces, 196*, Article 111339. https://doi.org/10.1016/j.colsurfb.2020.111339

Phlicharoenphon, W., Gritsanapan, W., Peungvicha, P., & Sithisarn, P. (2018). Determination of antioxidant activity, inhibitory effect if glucose absorption and acute toxicity of *Scaphium scaphigerum* fruit gel powder. *Journal of Health Research, 31*, 289–296. https://doi.org/10.14456/jhr.2017.36

Qiu, L., Zhang, M., Adhikari, B., & Chang, L. (2023). Microencapsulation of rose essential oil using perilla protein isolated-sodium alginate complex coacervates and application of microcapsules to preserve ground beef. *Food and Bioprocess Technology, 16*, 368–381. https://doi.org/10.1007/s11947-022-02944-8

Ramdhan, T., Ching, S. H., Prakash, S., & Bhandari, B. (2020). Physical and mechanical properties of alginate based composite gels. *Trends in Food Science & Technology, 106*, 150–159. https://doi.org/10.1016/j.tifs.2020.10.002

Rezvanian, M., Ahmad, N., Amin, M. C. I. M., & Ng, S. F. (2017). Optimization, characterization, and *in vitro* assessment of alginate-pectin ionic cross-linked hydrogel film for wound dressing applications. *International Journal of Biological Macromolecules, 97*, 131–140. https://doi.org/10.1016/j.ijbiomac.2016.12.079

Silva, S. D., Feliciano, R. P., Boas, L. V., & Bronze, M. R. (2014). Application of FTIR-ATR to Moscatel dessert wines for prediction of total phenolic and flavonoid contents and antioxidant capacity. *Food Chemistry, 50*, 489–493. https://doi.org/10.1016/j.foodchem.2013.11.028

Singleton, V., & Rossi, J. (1965). Colorimetry of total phenolic compounds with phosphomolybdic-phosphotungstic acid reagents. *American Journal of Enology and Viticulture, 16*, 144–158. https://doi.org/10.5344/ajev.1965.16.3.144

Srichamroen, A., & Chavasit, V. (2011a). *In vitro* retardation of glucose diffusion with gum extracted from Malva nut seeds produced in Thailand. *Food Chemistry, 127*, 455–460. https://doi.org/10.1016/j.foodchem.2010.12.153

Srichamroen, A., & Chavasit, V. (2011b). Rheological properties of extracted malva nut gum (*Scaphium scaphigerum*) in different conditions of solvent. *Food Hydrocolloids, 25*, 444–450. https://doi.org/10.1016/j.foodhyd.2010.07.016

Sun, Y., Hou, S., Song, S., Zhang, B., Ai, C., Chen, X., & Liu, N. (2018). Impact of acidic, water and alkaline extraction on structural features, antioxidant activities of *Laminaria japonica* polysaccharides. *International Journal of Biological Macromolecules, 112*, 985–995. https://doi.org/10.1016/j.ijbiomac.2018.02.066

Tiamiyu, Q. O., Adebayo, S. E., & Yusuf, A. A. (2023). Gum Arabic edible coating and its application in preservation of fresh fruit and vegetable: A review. *Food Chemistry Advances, 2*, Article 100251. https://doi.org/10.1016/j.focha.2023.100251

Tu, L., He, Y., Yang, H., Wu, Z., & Yi, L. (2015). Preparation and characterization of alginate–gelatin microencapsulated *Bacillus subtilis* SL-13 by emulsification/internal gelation. *Journal of Biomaterials Science, Polymer Edition, 26*, 735–749. https://doi.org/10.1080/09205063.2015.1056075

Wang, Q. C., Zhao, X., Pu, J. H., & Luan, X. H. (2016). Influences of acidic reaction and hydrolytic conditions on monosaccharide composition analysis of acidic, neutral and basic polysaccharides. *Carbohydrate Polymers, 143*, 296–300. https://doi.org/10.1016/j.carbpol.2016.02.023

Wani, A. A., Wani, I. A., Hussain, P. R., Gani, A., Wani, T. A., & Masoodi, F. A. (2015). Physicochemical properties of native and g-irradiated wild arrowhead (*Sagittaria sagittifolia* L.) tube starch. *International Journal of Biological Macromolecules, 77*, 360–368. https://doi.org/10.1016/j.ijbiomac.2015.03.012

Wongverawattanakul, C., Suklaew, P., Chusuk, C., Adisakwattana, S., & Thilavech, T. (2022). Encapsulation of Mesona chinensis benth extract in alginate beads enhances the stability and antioxidant activity of polyphenols under simulated gastrointestinal digestion. *Foods (Basel, Switzerland), 11*, Article 23778. https://doi.org/10.3390/foods11152378

Yadav, I., Purohit, S. D., Singh, H., Das, N., Roy, P., & Mishra, N. C. (2021). A highly transparent tri-polymer complex *in situ* hydrogel of HA collagen and four-arm-PEG as potential vitreous substitute. *Biomedical Materials, 16*, Article 065018. https://doi.org/10.1088/1748-605X/ac2714

Ying, Z., Han, X., & Li, J. (2011). Ultrasound-assisted extraction of polysaccharides from mulberry leaves. *Food Chemistry, 127*, 1273–1279. https://doi.org/10.1016/j.foodchem.2011.01.083

Zhang, Y., Zheng, W., Gu, J. F., Ni, J., Wang, L., Tang, Z. X., & Shi, L. E. (2015). Soy protein isolate-alginate microspheres for encapsulation of *Enterococcus faecalis* HZNU P2. *Brazilian Archives of Biology and Technology, 58*, 805–811. https://doi.org/10.1590/S1516